

# High-power, broadly tunable, and low-quantum-defect $\text{KGd}_{1-x}\text{Lu}_x(\text{WO}_4)_2:\text{Yb}^{3+}$ channel waveguide lasers

Dimitri Gekus,\* Shanmugam Aravazhi, Kerstin Wörhoff, and Markus Pollnau

Integrated Optical Microsystems Group, MESA<sup>+</sup> Institute for Nanotechnology, University of Twente,  
P.O. Box 217, 7500 AE Enschede, Netherlands

\*d.gekus@ewi.utwente.nl

**Abstract:** In  $\text{KGd}_{1-x}\text{Lu}_x(\text{WO}_4)_2:\text{Yb}^{3+}$  channel waveguides grown onto  $\text{KY}(\text{WO}_4)_2$  substrates by liquid phase epitaxy and microstructured by Ar<sup>+</sup> beam etching, we produced 418 mW of continuous-wave output power at 1023 nm with a slope efficiency of 71% and a threshold of 40 mW of launched pump power at 981 nm. The degree of output coupling was 70%. By grating tuning in an extended cavity and pumping at 930 nm, we demonstrated laser operation from 980 nm to 1045 nm. When pumping at 973 nm, lasing at 980 nm with a record-low quantum defect of 0.7% was achieved.

©2010 Optical Society of America

OCIS codes: (140.3615) Lasers, Ytterbium; (230.7380) Waveguides, channeled.

## References and links

1. J. R. Lee, H. J. Baker, G. J. Friel, G. J. Hilton, and D. R. Hall, "High-average-power Nd:YAG planar waveguide laser that is face pumped by 10 laser diode bars," *Opt. Lett.* **27**(7), 524–526 (2002).
2. J. Siebenmorgen, T. Calmano, K. Petermann, and G. Huber, "Highly efficient Yb:YAG channel waveguide laser written with a femtosecond-laser," *Opt. Express* **18**(15), 16035–16041 (2010).
3. J. D. B. Bradley, R. Stoffer, L. Agazzi, F. Ay, K. Wörhoff, and M. Pollnau, "Integrated  $\text{Al}_2\text{O}_3:\text{Er}^{3+}$  ring laser on silicon with wide wavelength selectivity," *Opt. Lett.* **35**(1), 73–75 (2010).
4. D. Pudo, H. Byun, J. Chen, J. Sickler, F. X. Kärtner, and E. P. Ippen, "Scaling of passively mode-locked soliton erbium waveguide lasers based on slow saturable absorbers," *Opt. Express* **16**(23), 19221–19231 (2008).
5. E. H. Bernhardt, H. A. G. M. van Wolferen, L. Agazzi, M. R. H. Khan, C. G. H. Roeloffzen, K. Wörhoff, M. Pollnau, and R. M. de Ridder, "Ultra-narrow-linewidth, single-frequency distributed feedback waveguide laser in  $\text{Al}_2\text{O}_3:\text{Er}^{3+}$  on silicon," *Opt. Lett.* **35**(14), 2394–2396 (2010).
6. J. Yang, M. B. J. Diemeer, C. Grivas, G. Sengo, A. Driessen, and M. Pollnau, "Steady-state lasing in a solid polymer," *Laser Phys. Lett.* **7**(9), 650–656 (2010).
7. M. Pollnau, Y. E. Romanyuk, F. Gardillou, C. N. Borca, U. Griebner, S. Rivier, and V. Petrov, "Double tungstate lasers: From bulk toward on-chip integrated waveguide devices," *IEEE J. Sel. Top. Quantum Electron.* **13**(3), 661–671 (2007).
8. A. A. Kaminskii, A. F. Konstantinova, V. P. Orekhova, A. V. Butashin, R. F. Klevtsova, and A. A. Pavlyuk, "Optical and nonlinear laser properties of the  $\chi^{(3)}$ -active monoclinic  $\alpha$ - $\text{KY}(\text{WO}_4)_2$  crystals," *Crystallogr. Rep.* **46**(4), 665–672 (2001).
9. N. V. Kuleshov, A. A. Lagatsky, A. V. Podlipensky, V. P. Mikhailov, and G. Huber, "Pulsed laser operation of Yb-doped  $\text{KY}(\text{WO}_4)_2$  and  $\text{KGd}(\text{WO}_4)_2$ ," *Opt. Lett.* **22**(17), 1317–1319 (1997).
10. K. Petermann, D. Fagundes-Peters, J. Johannsen, M. Mond, V. Peters, J. J. Romero, S. Kutovoi, J. Speiser, and A. Giesen, "Highly Yb-doped oxides for thin-disc lasers," *J. Cryst. Growth* **275**(1-2), 135–140 (2005).
11. R. Solé, V. Nikolov, X. Ruiz, J. Gavalda, X. Solans, M. Aguiló, and F. Díaz, "Growth of  $\beta$ - $\text{KGd}_{1-x}\text{Nd}_x(\text{WO}_4)_2$  single crystals in  $\text{K}_2\text{W}_2\text{O}_7$  solvents," *J. Cryst. Growth* **169**(3), 600–603 (1996).
12. S. Rivier, X. Mateos, Ö. Silvestre, V. Petrov, U. Griebner, M. C. Pujol, M. Aguiló, F. Díaz, S. Vernay, and D. Rytz, "Thin-disk Yb:KLu( $\text{WO}_4$ )<sub>2</sub> laser with single-pass pumping," *Opt. Lett.* **33**(7), 735–737 (2008).
13. B. Jacobsson, J. E. Hellström, V. Pasiskevicius, and F. Laurell, "Widely tunable Yb:KYW laser with a volume Bragg grating," *Opt. Express* **15**(3), 1003–1010 (2007).
14. S. Pekarek, C. Fiebig, M. C. Stumpf, A. E. H. Oehler, K. Paschke, G. Erbert, T. Südmeyer, and U. Keller, "Diode-pumped gigahertz femtosecond Yb:KGW laser with a peak power of 3.9 kW," *Opt. Express* **18**(16), 16320–16326 (2010).
15. B. Jacobsson, "Experimental and theoretical investigation of a volume-Bragg-grating-locked Yb:KYW laser at selected wavelengths," *Opt. Express* **16**(9), 6443–6454 (2008).
16. Y. E. Romanyuk, C. N. Borca, M. Pollnau, S. Rivier, V. Petrov, and U. Griebner, "Yb-doped  $\text{KY}(\text{WO}_4)_2$  planar waveguide laser," *Opt. Lett.* **31**(1), 53–55 (2006).

17. S. Rivier, X. Mateos, V. Petrov, U. Griebner, Y. E. Romanyuk, C. N. Borca, F. Gardillou, and M. Pollnau, "Tm:KY(WO<sub>4</sub>)<sub>2</sub> waveguide laser," *Opt. Express* **15**(9), 5885–5892 (2007).
18. F. M. Bain, A. A. Lagatsky, S. V. Kurilchick, V. E. Kisel, S. A. Guretsky, A. M. Luginets, N. A. Kalanda, I. M. Kolesova, N. V. Kuleshov, W. Sibbett, and C. T. A. Brown, "Continuous-wave and Q-switched operation of a compact, diode-pumped Yb<sup>3+</sup>:KY(WO<sub>4</sub>)<sub>2</sub> planar waveguide laser," *Opt. Express* **17**(3), 1666–1670 (2009).
19. F. M. Bain, A. A. Lagatsky, R. R. Thomson, N. D. Psaila, N. V. Kuleshov, A. K. Kar, W. Sibbett, and C. T. A. Brown, "Ultrafast laser inscribed Yb:KGd(WO<sub>4</sub>)<sub>2</sub> and Yb:KY(WO<sub>4</sub>)<sub>2</sub> channel waveguide lasers," *Opt. Express* **17**(25), 22417–22422 (2009).
20. F. Gardillou, Y. E. Romanyuk, C. N. Borca, R. P. Salathé, and M. Pollnau, "Lu, Gd codoped KY(WO<sub>4</sub>)<sub>2</sub>:Yb epitaxial layers: towards integrated optics based on KY(WO<sub>4</sub>)<sub>2</sub>," *Opt. Lett.* **32**(5), 488–490 (2007).
21. D. Geskus, S. Aravazhi, E. Bernhardt, C. Grivas, S. Harkema, K. Hametner, D. Günther, K. Wörhoff, and M. Pollnau, "Low-threshold, highly efficient Gd<sup>3+</sup>, Lu<sup>3+</sup> co-doped KY(WO<sub>4</sub>)<sub>2</sub>:Yb<sup>3+</sup> planar waveguide lasers," *Laser Phys. Lett.* **6**(11), 800–805 (2009).
22. D. Geskus, S. Aravazhi, C. Grivas, K. Wörhoff, and M. Pollnau, "Microstructured KY(WO<sub>4</sub>)<sub>2</sub>:Gd<sup>3+</sup>, Lu<sup>3+</sup>, Yb<sup>3+</sup> channel waveguide laser," *Opt. Express* **18**(9), 8853–8858 (2010).
23. M. Pujol, X. Mateos, R. Solé, J. Massons, J. Gavalda, F. Díaz, and M. Aguiló, "Linear thermal expansion tensor in KRE(WO<sub>4</sub>)<sub>2</sub> (RE = Gd, Y, Er, Yb) monoclinic crystals," *Mater. Sci. Forum* **378–381**, 710–717 (2001).
24. M. Pujol, X. Mateos, A. Aznar, X. Solans, S. Suriñach, J. Massons, F. Díaz, and M. Aguiló, "Structural redetermination, thermal expansion and refractive indices of KLu(WO<sub>4</sub>)<sub>2</sub>," *J. Appl. Crystallogr.* **39**(2), 230–236 (2006).
25. C. Grivas, D. P. Shepherd, T. C. May-Smith, R. W. Eason, M. Pollnau, A. Crunteanu, and M. Jelinek, "Performance of Ar<sup>2+</sup>-milled Ti:Sapphire rib waveguides as single transverse mode broadband fluorescence sources," *IEEE J. Quantum Electron.* **39**(3), 501–507 (2003).

## 1. Introduction

In the coming years, many applications in photonics will take advantage of miniaturization by on-chip integration of optical components, may it be for biomolecule detection and manipulation, optical coherence tomography or Raman spectroscopy, trace-gas detection, atom spectroscopy, optical clocks, optical computing, data communication, or laser beam steering, to name a few. In most applications, high-performance integrated lasers are required that provide high output power [1] and efficiency [2], excellent beam quality, broad wavelength selectivity [3] and tunability, ultrashort pulses [4], ultra-narrow bandwidth [5], or ultra-low heat generation, potentially by applying a low-cost, straight-forward fabrication process [6].

The potassium double tungstates KGd(WO<sub>4</sub>)<sub>2</sub>, KY(WO<sub>4</sub>)<sub>2</sub>, and KLu(WO<sub>4</sub>)<sub>2</sub> are excellent candidates for solid-state lasers [7] because of their high refractive index of ~2.0–2.1 [8], the large transition cross-sections of rare-earth (RE) ions doped into these hosts [9], a long inter-ionic distance of ~0.5 nm that allows for large doping concentrations without lifetime quenching [10], and a reasonably large thermal conductivity of ~3.3 W m<sup>-1</sup> K<sup>-1</sup> [11]. These advantages have been exploited to demonstrate thin-disk lasers [12], broadly tunable [13] and high-energy ultrashort-pulse lasers [14], low-quantum-defect lasers [15], as well as planar [16–18] and channel [19] waveguide lasers. Co-doping of grown KY(WO<sub>4</sub>)<sub>2</sub>:RE thin films with Gd and Lu ions for lattice matching and enhanced refractive index contrast of up to 7.5 × 10<sup>-3</sup> with respect to the undoped KY(WO<sub>4</sub>)<sub>2</sub> substrate [20] has enabled waveguide lasers with tight pump and laser mode confinement of ~10 μm<sup>2</sup>, resulting in excellent slope efficiencies in Yb-doped planar and microstructured channel waveguide lasers of 82.3% [21] and 62% [22], respectively.

In this work we fabricate a double tungstate microstructured channel waveguide with further enhanced refractive index contrast of 1.5% and demonstrate a laser with an output power of 418 mW at 1023 nm, limited only by the available pump power. The obtained slope efficiency of 71% versus launched pump power is, to the best of our knowledge, the highest value reported for a dielectric channel waveguide laser with unidirectional output. In two other resonator configurations, broad tunability of the laser wavelength from 980 to 1045 nm as well as a record-low quantum defect of 0.7% when pumping at 973 nm and lasing at 980 nm is obtained, thereby minimizing heat dissipation in the device. These results show a great potential of double tungstate channel waveguide lasers to excellently fulfill many of the aforementioned requirements.

## 2. Sample fabrication

The composition of the active layer was chosen to provide the maximum refractive index contrast and simultaneously minimal lattice mismatch with the  $\text{KY}(\text{WO}_4)_2$  substrate. The lattice parameters [23, 24] of the  $a$  and  $c$  crystallographic axes within the plane of the monoclinic layer were calculated as weighted averages of the lattice parameters of the stoichiometric compositions  $\text{KGd}(\text{WO}_4)_2$ ,  $\text{KLu}(\text{WO}_4)_2$ , and  $\text{KYb}(\text{WO}_4)_2$  and were matched to the parameters of the  $\text{KY}(\text{WO}_4)_2$  substrate. No  $\text{Y}^{3+}$  was incorporated in the active layer in order to achieve a maximal refractive index contrast of 1.5% between layer and substrate. A  $\text{KGd}_{0.49}\text{Lu}_{0.485}\text{Yb}_{0.025}(\text{WO}_4)_2$  layer was grown by liquid phase epitaxy onto an undoped, (010)-orientated, laser-grade polished  $\text{KY}(\text{WO}_4)_2$  substrate of  $1\text{ cm}^2$  size in a  $\text{K}_2\text{W}_2\text{O}_7$  solvent [11] at temperatures of  $920\text{--}923^\circ\text{C}$ . Subsequently, the layer surface was polished parallel to the layer-substrate interface to a uniform thickness of  $5\text{ }\mu\text{m}$  with a measured rms surface roughness of  $1.5\text{ nm}$ . A photoresist (908/35) mask was deposited and patterned by lithographic steps. These patterns were then transferred by  $\text{Ar}^+$  beam milling [25] to obtain  $1.4\text{-}\mu\text{m}$ -deep ridge waveguides along the  $N_g$  optical axis, with a channel width of  $7\text{ }\mu\text{m}$  [22]. The structure was overgrown by an epitaxial layer of  $\text{KY}(\text{WO}_4)_2$ , resulting in buried channel waveguides with a length of  $6.6\text{ mm}$ , which guide only the fundamental mode around  $1\text{ }\mu\text{m}$ . The  $\text{KY}(\text{WO}_4)_2$  overlay reduces the propagation losses, improves the mode overlap with the active region, and simplifies endface polishing.

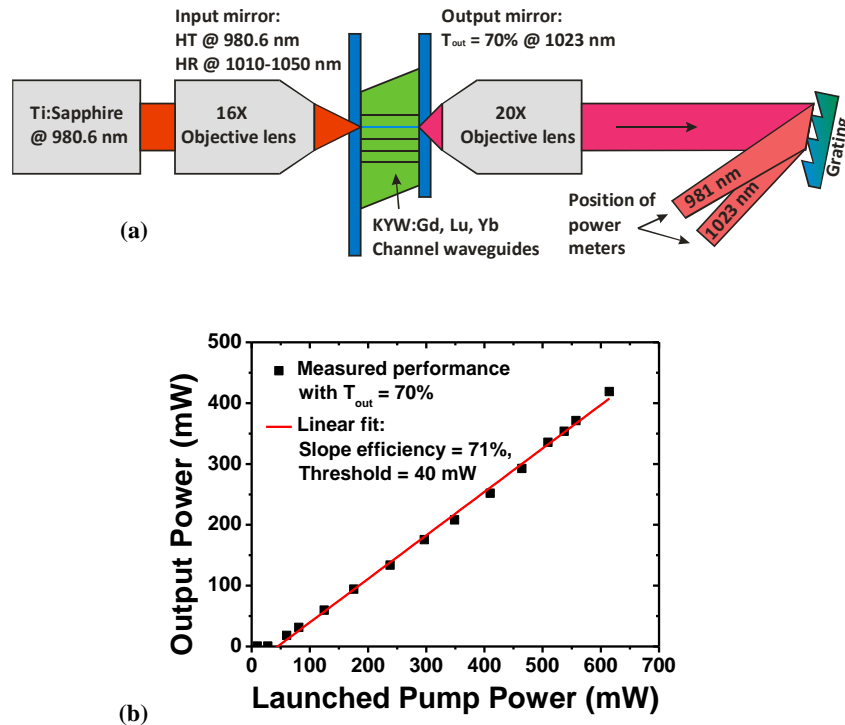


Fig. 1. (a) Experimental setup for high laser output power; (b) input-output curve of the  $\text{KGd}_{1-x}\text{Lu}_x\text{W:Yb}^{3+}$  channel waveguide laser pumped at 981 nm and lasing at 1023 nm.

## 3. Laser experiments

The sample was placed on an aluminum mount without active cooling, thus indicating room for further power scaling. Pump light at 980.6 nm from a broadly tunable Ti:sapphire laser was end-coupled by a  $\times 16$  microscope objective into the waveguide. The light outcoupled at the other end of the waveguide was collimated by a  $\times 20$  microscope objective. A reflective

grating was used to separate the residual transmitted pump power from the laser emission and the laser light was directed to a powermeter or a spectrometer. At the input side a dielectric mirror with a high transmission of  $T = 96\%$  for the pump light and a high reflectivity of  $R = 99.8\%$  for the laser light was directly butt-coupled to the endfacet with fluorinated oil (Fluorinert FC70). An outcoupling mirror with  $T_{out} = 70\%$  at 1023 nm was attached to the other side. A schematic of the experimental setup is shown in Fig. 1(a). We obtained a maximum laser output power of 418 mW at 1023 nm, limited only by the available pump power, with a slope efficiency of 71% versus launched pump power; see Fig. 1(b). The threshold was 40 mW. Almost no residual pump light was observed at the output, as 99% of the launched pump power was absorbed in the slightly too long waveguide.

To achieve broad wavelength tunability of the laser output, an incoupling mirror with  $\sim 99.8\%$  reflectivity from 980 nm to 1050 nm was attached to the incoupling side. The transmission of this mirror steeply increased below 932 nm, hence a short pump wavelength of 930 nm was chosen. The outcoupling mirror was removed and the cavity extended by collimating the output with a  $\times 20$  microscope objective and directing it onto a grating (576 l/mm, blazed at  $23.5^\circ$ ) in Littrow configuration to provide strongly wavelength-selective feedback. A schematic of the experimental setup is shown in Fig. 2(a).

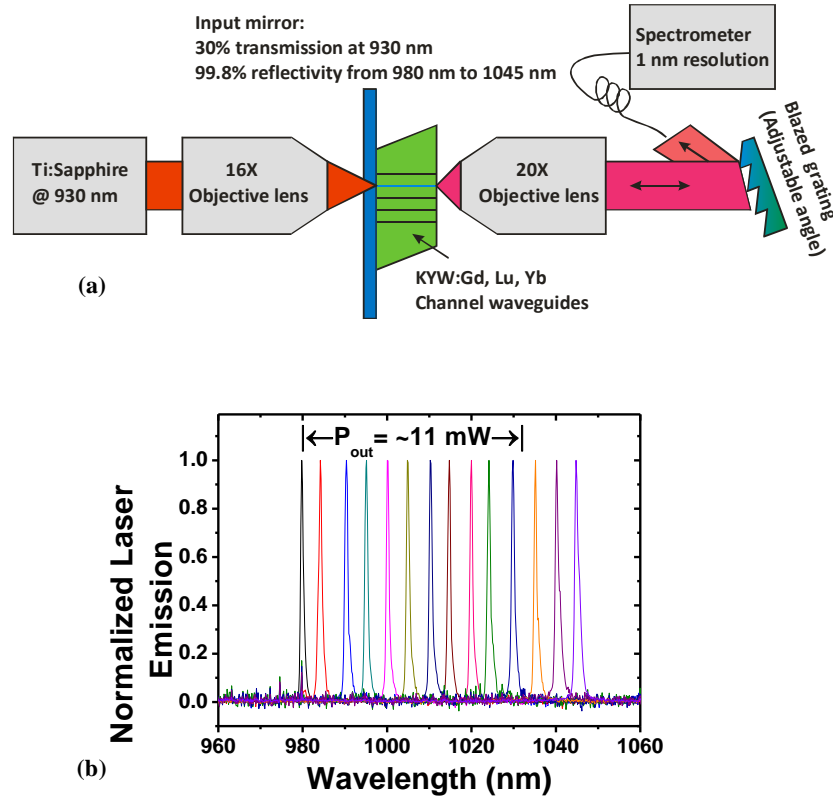


Fig. 2. (a) Experimental setup for tuning the laser emission by extension of the cavity with a reflective grating in Littrow configuration; (b) measured emission spectra under pumping at 930 nm when changing the angle of the reflective grating.

By rotation of the grating the emission wavelength could be continuously tuned from 980 nm to 1045 nm; see Fig. 2(b). With 120 mW of launched pump power at 930 nm, output powers of approximately 11 mW were measured from the 2<sup>nd</sup> order of the grating in the wavelength range 980-1033 nm. The emission dropped gradually when tuning the laser to 1045 nm, followed by operation at 980 nm when further rotating the grating. The intracavity

loss in this experiment is estimated to be up to 50% due to non-optimal optical elements, therefore the threshold is high and the slope efficiency small. An even larger tuning range, extended towards longer wavelengths, is expected in cavities with lower loss [15].

In a third experiment, laser operation with a record-low quantum defect was demonstrated. The mirror at the incoupling side was removed, and a mirror with a reflectivity of 97% at 980 nm was butt-coupled to the other waveguide end. In this situation, laser emission at a wavelength of 980 nm was extracted from the pumped side. The experimental setup is shown in Fig. 3(a). Remarkably, the laser continuously oscillated at 980 nm while tuning the excitation wavelength from 910 nm to 973 nm. The spectrum in the latter pump-wavelength setting is displayed in Fig. 3(b), resulting in a record-low quantum defect of only 0.7%.

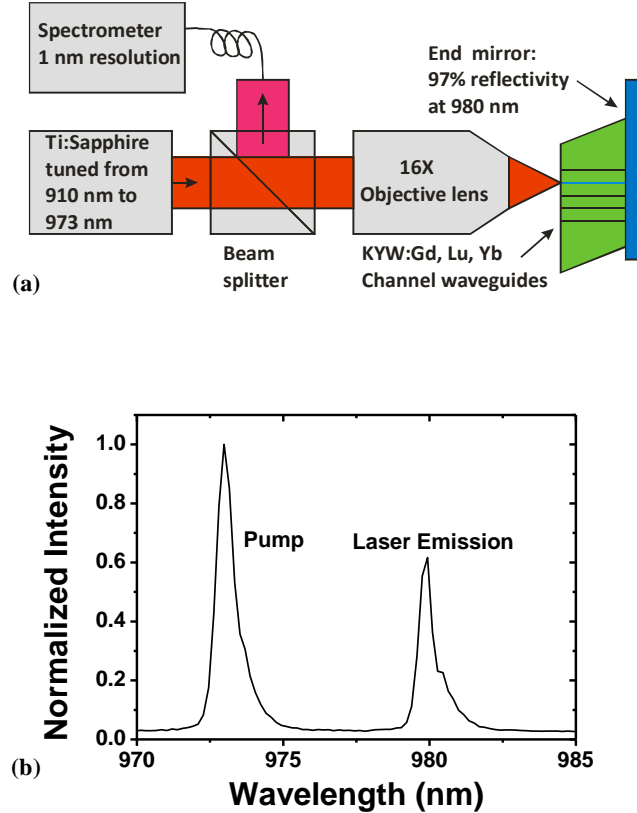


Fig. 3. (a) Experimental laser setup for the demonstration of low-quantum-defect lasing; (b) spectrum recorded during lasing with the smallest attained quantum defect.

#### 4. Conclusions

The remarkable performance of such a rare-earth-ion-doped, microstructured channel waveguide laser demonstrated in this paper has enormous consequences. Firstly, the large bandwidth, combined with a short cavity length and very high laser intensity oscillating in the waveguide, make this device an excellent candidate for high-repetition-rate ultrashort-pulse generation on a chip. Secondly, when replacing a large part of the  $\text{Lu}^{3+}$  ions with  $\text{Yb}^{3+}$  ions of almost the same ionic radius in the active layer, the absorption length at 980 nm can be reduced to much less than 100  $\mu\text{m}$ , allowing one to move from a single-mode-diode end-pumping to a diode-array side-pumping configuration. Such a side-pumped scheme, combined with an ultra-low quantum defect and accordingly small heat generation, promises to be a great step forward toward efficient integrated waveguide lasers emitting large single-

mode output powers far beyond 1 W. Thirdly, integrated distributed feedback (DFB) waveguide lasers without active wavelength stabilization have recently produced a linewidth of 1.7 kHz at 3 mW of output power [5]. The linewidth narrows linearly as the laser power increases, hence the output power obtained in this work would bring about a DFB laser with an ultra-narrow linewidth in the range of 10-20 Hz. The minimal thermal load is also of great advantage for the wavelength stability of such ultra-narrow linewidth lasers.

### **Acknowledgments**

The authors acknowledge financial support by The Netherlands Organization for Scientific Research (NWO) through the VICI Grant no. 07207 "Photonic integrated structures".